

Fig. S1. Body and wing kinematic time series from one of the analyzed escape manoeuvres of the magnificent hummingbird. Vertical grey stripes indicate downstrokes.

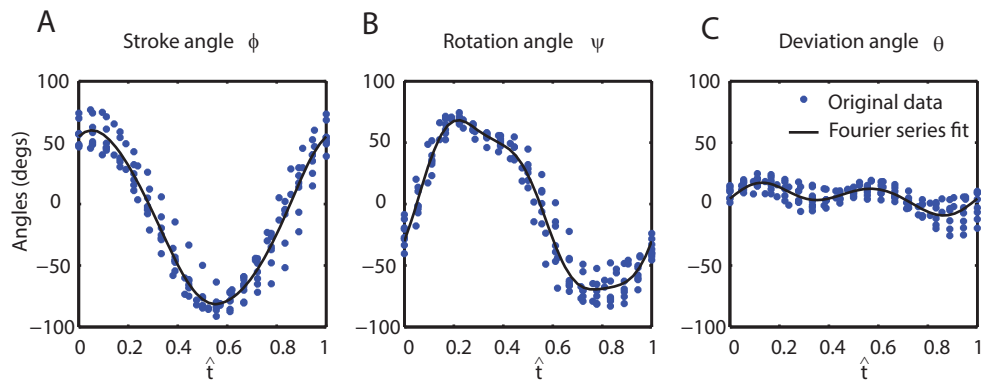


Fig. S2. An example of original Euler angle data points and Fourier series parameterized Euler angles for the hovering wing kinematics of black-chinned hummingbirds.

Table S1. Interspecific correlations between stroke-averaged kinematic variables and body angular velocities (roll, pitch and yaw) which were statistically significant ($P < 0.05$). Superscripts u and d represent upstroke and downstroke, subscripts l and r represent left and right wings. U is wing tip velocity, θ is wing deviation angle, ψ is wing rotation angle, α is wing angle of attack, β is wing stroke plane tilt angle, n is wingbeat frequency, and ϕ is wing stroke position angle.

	Body roll	Body pitch	Body yaw
Observed in all species	$\overline{\theta_l - \theta_r}^d$	$\overline{(U_l + U_r)/2}^{u,d}$	$\overline{\theta_l - \theta_r}^u$
	$\overline{\psi_l - \psi_r}^d$	$\overline{(n_l + n_r)/2}^d$	$\overline{\psi_l - \psi_r}^u$
	$\overline{\alpha_l - \alpha_r}^d$		
Stroke-averaged kinematic variables			$\overline{\beta_l - \beta_r}^{u,d}$
Observed in three species	$\overline{U_l - U_r}^d$	$\overline{(\psi_l + \psi_r)/2}^d$	$\overline{\theta_l - \theta_r}^d$
	$\overline{\beta_l - \beta_r}^d$	$\overline{(\beta_l + \beta_r)/2}^d$	
		$\overline{(\theta_l + \theta_r)/2}^u$	$\overline{\phi_l - \phi_r}^d$

Table S2. Correlations between wing kinematic parameters and pitch rate during downstroke for each species.

Species	Bilateral symmetric change of wing rotation $(\psi_l + \psi_r)/2$		Bilateral symmetric change of wing velocity $(U_l + U_r)/2$		Bilateral symmetric change of stroke plane angle $(\beta_l + \beta_r)/2$		Bilateral symmetric change of wingbeat frequency $(n_l + n_r)/2$	
	P	ρ	P	ρ	P	ρ	P	ρ
Blue-throated hummingbird, (<i>Lampornis clemenciae</i>)	n.s.	0.19	<0.0001	-0.77	n.s.	0.22	<0.0001	-0.70
Magnificent hummingbird (<i>Eugenes fulgens</i>)	0.0038	0.55	<0.0001	-0.69	0.0080	0.51	<0.0001	-0.69
Black-chinned hummingbird, (<i>Archilochus alexandri</i>)	0.0022	0.50	<0.0001	-0.69	0.0026	0.49	<0.0001	-0.76
Broad-billed hummingbird (<i>Cynanthus latirostris</i>)	0.0002	0.63	0.0004	-0.61	0.0003	0.62	0.0002	-0.62

Table S3. Wing kinematic parameters correlated with roll rate during downstroke for each species.

Species	Bilateral asymmetry of wing deviation $\overline{\theta_l - \theta_r}$		Bilateral asymmetry of wing rotation $\overline{\psi_l - \psi_r}$		Bilateral asymmetry of wing angle of attack $\overline{\alpha_l - \alpha_r}$		Bilateral asymmetry of wing velocity $\overline{U_l - U_r}$	
	P	ρ	P	ρ	P	ρ	P	ρ
Blue-throated hummingbird, (<i>Lampornis clemenciae</i>)	<0.0001	0.72	<0.0001	-0.71	<0.0001	0.75	0.012	0.45
Magnificent hummingbird (<i>Eugenes fulgens</i>)	<0.0001	0.86	0.0017	-0.58	0.0061	0.52	n.s.	0.31
Black-chinned hummingbird, (<i>Archilochus alexandri</i>)	0.0010	0.53	<0.0001	-0.68	<0.0001	0.67	<0.0001	0.65
Broad-billed hummingbird (<i>Cynanthus latirostris</i>)	0.0004	0.60	<0.0001	-0.67	0.0003	0.61	0.025	0.41

Table S4. Wing kinematic parameters correlated with yaw rate during upstroke.

Species	Bilateral asymmetric change of wing rotation $\overline{\psi_l - \psi_r}$	
	P	ρ
Blue-throated hummingbird, (<i>Lampornis clemenciae</i>)	0.012	-0.48
Magnificent hummingbird (<i>Eugenes fulgens</i>)	0.040	-0.42
Black-chinned hummingbird, (<i>Archilochus alexandri</i>)	0.002	-0.52
Broad-billed hummingbird (<i>Cynanthus latirostris</i>)	0.020	-0.44